Sliding mode controlled PV-based bootstrap converter system with enhanced response and voltage stability

Kesa Jyothi[1], Pinni Srinivasa Varma[1], Dondapati Ravi Kishore[2], Hari Shankar Jain[3]
[1]Department of Electrical and Electronics Engineering, Koneru Lakshmaiah Education Foundation, Guntur, India
[2]Department of Electrical and Electronics Engineering, Godavari Institute of Engineering and Technology, Rajahmundry, India
[3]Department of Electrical and Electronics Engineering, Vardhaman College of Engineering, Hyderabad, India

Article Info

ABSTRACT

In this paper, a straight forward method for locating the controller in a PV-based bootstrap converter system is presented. Recent developments in control strategies and power electronics have made it possible to create PV-based DC-to-AC converters for AC drives that are connected to 3-phase loads. High voltage gain is intended to be produced by the bootstrap converter (BSC). The BSC's purpose is to control load voltage. This study compares the time specification performance of the proportional resonant controller (PRC) and the sliding mode control (SMC) for photovoltaic systems with bootstrap three phase inverter (PV-BSTPI). For the delicate loads, steady voltage is typically more important. The BS-TPI system incorporates a closed loop control to fast achieve constant voltage. Choosing the best control approach is the aim. It is observed that the steady state error of SMC is 1.67 which is better when compared to PRC.
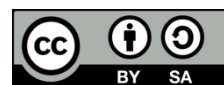
Corresponding Author:

Kesa Jyothi
Department of Electrical and Electronics Engineering, Koneru Lakshmaiah Education Foundation
Green Fields, Vaddeswaram, Guntur-522502, Andhra Pradesh, India
Email: jyothi11.eee@gmail.com

1. INTRODUCTION

Photovoltaic (PV) power is already nondeterministic due to its reliance on climatic and environmental variables. This creates significant challenges for diffusion and dispersion framework administrators as well as market administrators [1]. They are constantly required to regulate local creation that is unable to respond clearly to existing previous age repercussions. As a result, the impact of this vulnerability on organizational activities is severe. For example, huge edges of energy hold are important to have the choice to control the act of doing from earlier age plans, and the circulated energy assets of clever lattices should be managed under such vulnerability [2]. To attain such goals, projections of PV power for a specific time horizon should be available as early as a couple of days before the actual energy age. The essential writing on PV power gauging is extremely diverse. Most scientists and specialists use deterministic PV power estimation, which is the removal of a single value that predicts the true PV power at a specific time horizon [3]. Nonetheless, due to the inherent haphazardness of the real marvels, PV power gauging is best handled within probabilistic algorithms.

The technique of DC-DC conversion was first introduced in the 1920s. Initially, to obtain less voltage from the supply, a voltage divider or the use of variable resistance (rheostat) was attempted, which resulted in poor performance [4]. In addition, a multi-quadrant chopper for DC-DC conversion is being developed for industrial applications. As huge developments happened in the communication area, the requirement for low-voltage DC sources rose, resulting in extensive research in DC-DC converter topologies [5]. Initially, elementary circuit-based choppers were built for a few prototype models, and they met the

requirement. DC choppers are power electrical components that convert fixed DC voltage to variable DC voltage, hence the term DC-DC converters. According to their operation, converters are categorized as buck, boost, and buck-boost. Buck converters are used when the output voltage is less than the input voltage [6], whereas boost converters are used when the output voltage is greater than the input voltage. If the output voltage is larger than or less than the supply voltage, a Buck-boost converter is employed. The output voltage of Cuk converter is specified to be the inverse of the supplied voltage. It's also known as an inverting regulator [7]. The ON/OFF state of the switch controls the conversion ratio of these converters. DC-DC converters can now be operated at two different frequencies. One operates at high frequencies (10 kHz-1 MHz), while the other operates at lower frequencies. When the former is utilized at higher frequencies, the components L, C, and transformers become lighter and smaller in weight and size. The first is utilized for low and medium-power applications, while the second is used for high-power applications. The PWM technique [8] is used to turn on and off switches (IGBT or MOSFET). DC-DC converters are critical for maximizing the use of electricity from numerous sources. The output of the PV cell is quite low when dealing with grid-connected systems. To counteract this, boost converters are used to increase the output of PV cells. Traditional boost converters have disadvantages, such as slow switching and being unsuitable for high-power and high-temperature applications [9]. To improve the performance of DC-DC converters, enormous modifications have happened in the literature. Cascaded converters are made up of two converters connected back-to-back with additional switches. A quadratic boost converter (QBC) is an example of a cascaded converter with only one switch [10]. QBC is a novel topology that outperforms conventional in terms of efficiency, voltage gain, and keeping the same number of switches. As this converter injects less current ripple into the source, the efficiency and lifespan of PV arrays rise [11]. Theoretical high voltage gain for classical boost and buck-boost converters can be produced by using extreme duty cycles. Maximum attainable voltage gain is limited to roughly five in practice due to switch speed limitations, parasitic components, and power losses [12]. Because of the advancement of high-voltage gain converters, many DC-DC converters have been presented. Many studies have been conducted, for example, on high-gain topologies using stages [13] and magnetic coupling. In addition to the foregoing, quadratic gain converters were developed as an option.

A traditional boost converter is unsuitable for use in high-power industries where efficiency is critical because it has various switching characteristics that result in substantial I^2R losses [14]. As a result, a quadratic boost converter is constructed as a combination of two boost converters with only one active switch in the form of a MOSFET, resulting in lower losses and higher efficiency. QBC's limitations include unstable voltage regulation and low saturation points [15].

Low-duty cycle QBC is achieved with a high step-up and conversion ratio [16]. The expression for the conversion ratio is created, and the converter's switching operating circumstances are taken into account and expressed as quadratic equations [17]. To enhance power quality and manage overvoltage and current, the QBC employs the average current mode control. Researchers currently have a challenging task dealing with the extremely complex design of DC-DC converters with high voltage gain and minute output ripple waves [18]. To avoid the difficulties of output ripple waves and voltage transfer gain. In comparison to all other conventional DC-DC converters, KY converters have developed a superior converter. In terms of the power loss in the filter inductor, the power loss in the output capacitor, and the transient current over parasitic resistors, KY converters outperform boost converters [19]. KY converter is a non-isolated DC-DC boost converter that runs in continuous conduction mode and has a low output voltage ripple [20]. A KY boost converter is a hybrid of a KY converter and a synchronous rectifier converter. While functioning, traditional boost converters generate a high amount of output voltage ripple, which causes noise. An LC inductance filter or comparable series resistance capacitor is added to the existing circuit to overcome this and reduce output voltage ripple. To reduce output voltage ripple, several regulating techniques such as SMC, coupling inductor, loop bandwidth control, and voltage control techniques [21] are applied. In real-time applications, achieving one right-half plane zero with the aforementioned approaches running in continuous conduction mode (CCM) is extremely challenging. To address this KY boost converter with two modes of operation: charging and discharging, gives a very low output ripple in continuous conduction mode.

Although the number of commitments committed to probabilistic PV power anticipating is much lower than that in the deterministic structure, writing audits, and rivalry overviews reveal a changed cutting edge. These approaches are typically classified as boosting, stacking, and packing. Boosting comprises building a "solid" model by consolidating a few more vulnerable ones, which are prepared repetitively. Stacking is the process of combining the findings of several models that are treated in the same or similar manner to create the final forecast [22]. Packing entails constructing the final expectation as a combination of the output of a similar model run on multiple occasions, with input data resample via substitution (i.e., bootstrap totaled).

The emerging planar exchanged hesitance engine SMC for precise situating is appropriate for obstruction hiding [23]. To begin, the mechanical structure, framework structure, and numerical model with

realized boundaries obtained using a failing-to-recall factor recursive least-squares computation are presented in sequence [24]. At that point, the SMC's exchanging capacity and arriving at the law were resolved. The control law is also deduced for the SMC. The SMC's security is also shown using the Lyapunov steadiness hypothesis.

Existing studies do not propose a single architecture capable of achieving requirements such as high gain, a wide range of operations, and low ripple when integrating PV and AC drives. There is no performance comparison of the quadratic-boost converter [25], KY step-up converter, and bootstrap converter (BSC).Constant voltage is generally in higher demand for loads. Closed loop control is used in the circuit to fast achieve constant voltage for closed loop (CL) BC-TPI. The primary goal of this study is to find the best controller for a CL-BC-TPI utilized in constant voltage situations.

Pulse -width modulation (PWM) is the most used technique to control switching power supplies. The traditional PWM based power electronic circuits operates adaptively for a specific condition as they are modified based on averaging techniques. Nonlinear controller's offer a good large signal transient over linear controllers like P, PI, and PID as latter do not react immediately to transient conditions. One of the best nonlinear controllers for variable structure systems is slide mode control as these systems are robust to parameter variations and external disturbances. Accordingly, the switched-mode converters used in PV system applications are the ideal target of this kind of controller [26], [27]. Either it being a DC-DC converter or it being an inverter, the SMC has been used widely in the literature. Kim et al. applied the SM to control the inverter switches in order to force the followed current in the grid to pursue a generated reference current; the simulation and experimental results of this single-stage grid-connected PV system shown that the proposed controller can reduce current overshot and contribute to the optimal design of power devices [28]–[35].

This slide mode controller has a high degree of design flexibility and its comparatively easy to design. It is used in various industrial applications like automotive control and furnace control. The overwork is related to the sliding mode-controlled PV-based bootstrap converter-inverter system. Sliding mode-controlled PV-based bootstrap converter-inverter system is recommended in this endeavor. Sliding mode control is a nonlinear control technique used to modify the dynamics of a nonlinear system by causing it to "slide" over a cross-section of its typical behavior.

The document is laid out as follows: i) The topology of the CL-BC-TPI is presented in section 2 of the manuscript, and performance analysis using the Simulink model is shown in part 3; ii) Section 3 discusses the control strategies; iii) Section 4 reports on result analysis; and iv) Section 5 reports on the CL-BC-TPI conclusions derived from this research.

2. PROPOSED TOPOLOGY

Figure 1 shows a block diagram of a PR controlled closed loop bootstrap with a 3-phase inverter (BC-TPI). PV yield is focused on BC matching load voltage with PV voltage. The yield of the bootstrap converter is converted to alternating current (AC) by using a [8] three-phase inverter, which creates a constant frequency at the load. The load voltage is measured and compared to the reference voltage. The voltage PRC is oblivious to voltage inaccuracy [9]. The reference voltage is compared to the actual voltage, and the error is used by the PRC [10] to update the pulse width of the bootstrap converter and TPI. As a result, this system functions as a voltage-mode-controlled BC-TPI.

Figure 2 shows a block diagram of an SM-controlled-closed loop bootstrap with a 3-phase inverter. In Figure 1, the PRC has been switched out for the suggested SMC. The voltage of the load is changed, and this new voltage is compared to the reference voltage to determine the voltage error. The voltage inaccuracy is inferred from the voltage standard deviation. The reference voltage is matched with the actual voltage and the error is utilized to update the PWM of the Bootstrap converter and TPI.
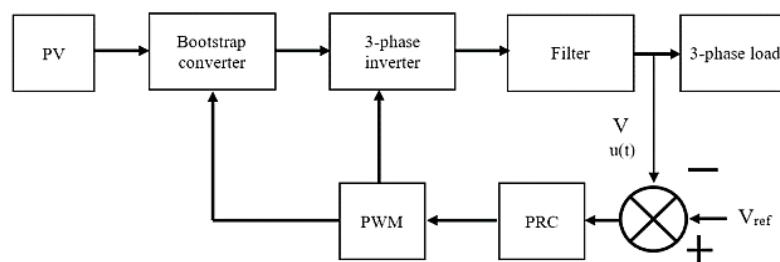

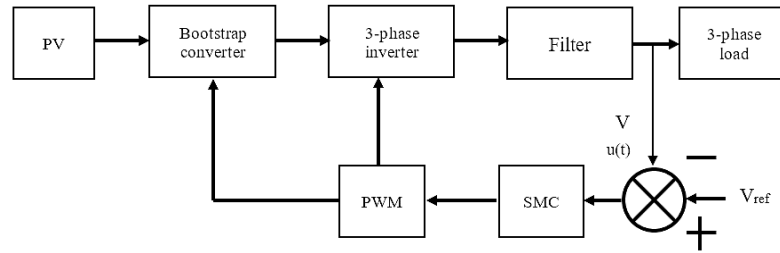Figure 1. Block diagram of PR controlled closed loop BC-TPI

Figure 2. Block diagram of SM controlled closed loop BC-TPI

The square of the error is integrated throughout the course of time by integral square error (ISE). Large errors will be punished more severely by ISE than smaller ones, due to the fact that the square of a large error will be a significantly larger value. Control systems that have been designed to minimize ISE will typically eliminate major errors rapidly, but they will allow little faults to continue for an extended length of time if they are allowed to do so. The controller input is given in (1). The controller input is given by (1).

$$u(t) = V_{ref} - V \hspace{4cm} (1)$$

Where $u(t)$ is the input to the controller, V_{ref} is the reference voltage and V is the voltage at the load side.

3. SIMULATION RESULTS

The projected controller performance is analyzed in this section in three cases. In case 1, the performance of BC-TPI is presented in an open loop system. In case 2, the performance of the BC-TPI is presented using the PRC [11]. The performance of BC-TPI is presented using the SMC in case 3.

− Case 1: Open loop BC-TPI with source disturbance

The circuit diagram [12], [13] of open-loop-BC-TPI with source disturbance is delineated in Figure 3. Figure 4 illustrates the voltage that is measured across the PV of the BC-TPI, and its value is 48 V [10]. Table 1 contains the parameters that will be used for the simulation. Figure 5 illustrates the voltage that is present across BC, and its value is 336 V. The value of the output voltage of the inverter when it is connected to an R-load is shown in Figure 6, and it is 280 V. Figure 7 illustrates the inverter's output current when it is connected to an R-load, which has a value of 1.2 A. Figure 8 illustrates the output power of the inverter with an R-load, which has been calculated to be 460 W.
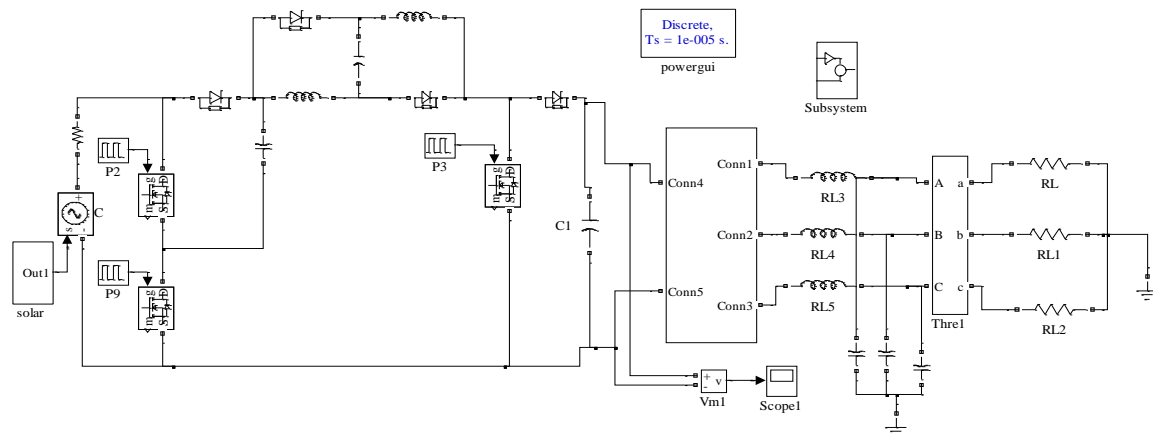
Figure 3. Circuit diagram of open-loop-BC-TPI

Table 1. Simulation parameters of BC-TPI

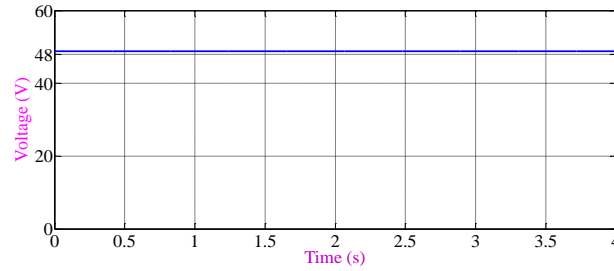| Parameters	Values
V_{in}	48 V
C_1	10 mF
L_1	0.5 mH
C_2, C_3	50 µF, 10 mF
L_2	3 µH

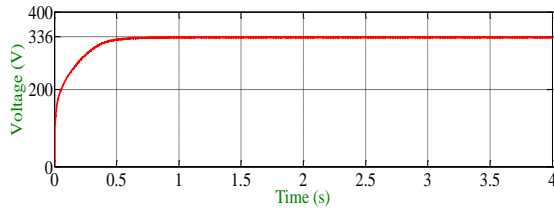Figure 4. Voltage across PV of BC-TPI in open-loop

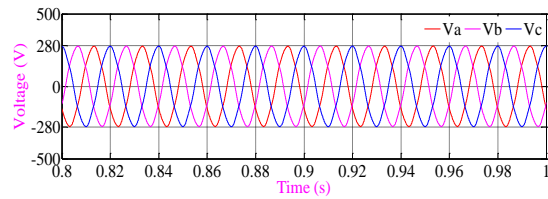Figure 5. Voltage across bootstrap converter in open-loop

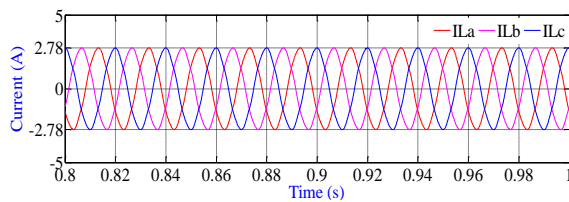Figure 6. Voltage across R–load of BC-TPI in open-loop

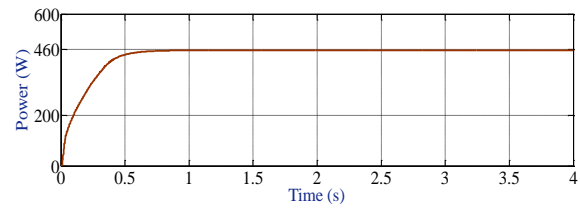Figure 7. Current through R–load of BC-TPI in open-loop

Figure 8. Output power of BC-TPI in open-loop

− Case 2: PR controlled closed loop BC-TPI

Figure 9 shows the circuit diagram for a PR controlled closed-loop BC-TPI with a 3-phase inverter [14]. To calculate the voltage error, the AC output of the TPI is first rectified and then compared to the reference voltage. The PRC receives the voltage error that was measured. To determine the voltage inaccuracy, the yield of PRC is compared with the actual voltage. To obtain an updated PWM for BSC, the voltage error is applied to the PRC. Figure 10 illustrates the voltage that is present across the PV of the BC-TPI, and its value is 58 V.

Figure 11 illustrates the voltage that is present across the TPI, and its value is 336 V. The value of the output voltage of the inverter when it is connected to R–load is shown in Figure 12 and is 280 V [15]. Figure 13 illustrates the output current of the inverter when it is connected to an R–load, and its value is 2.78 A. Figure 14 [16] illustrates the output power of the inverter when it is connected to an R-load, and its value is 460 W.

− Case 3: SM controlled closed loop bootstrap converter with 3phase inverter

The schematic representation of the SM-controlled closed-loop BC-TPI may be seen in Figure 15. The voltage fault is sent to the SMC so that an updated PWM can be generated for the BSC. Figure 16 illustrates the voltage that is measured across the PV [17] of the BC-TPI, and its value is 58V. Figure 17 illustrates the voltage that is present across the load of the TPI, and its value is 336 V.

Figure 18 illustrates the inverter's output voltage when it is connected to R–the load and the value of this voltage is 280 V. Figure 19 illustrates the output current of the inverter when it is connected to an R-load, and its value is 2.78 A [18]–[22]. Figure 20 illustrates the output power of the inverter with an R-load, which has been calculated to be 445 W.
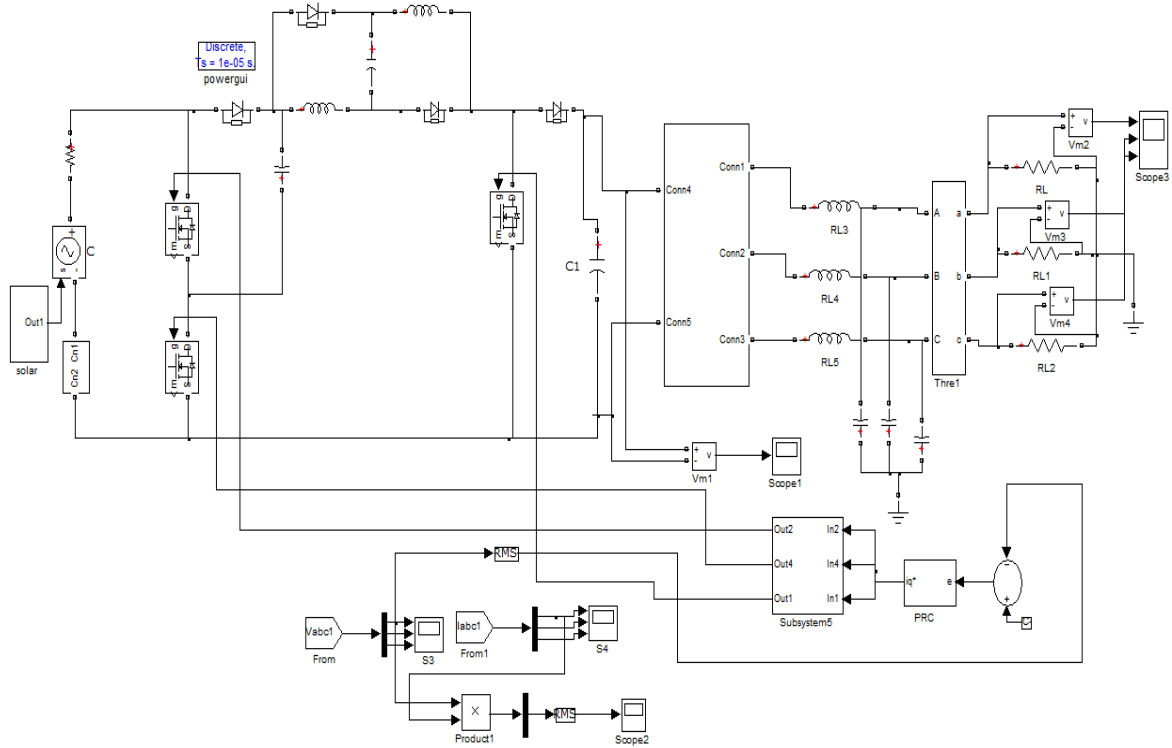
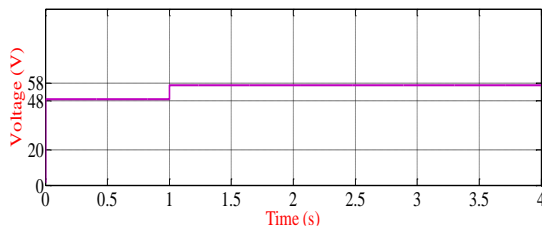Figure 9. Circuit diagram of PR controlled closed-loop BC-TPI
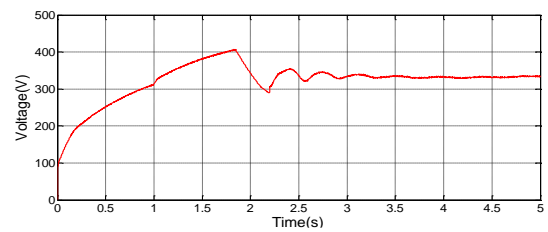

Figure 10. Voltage across PV of BC-TPI

Figure 11. Voltage across bootstrap converter
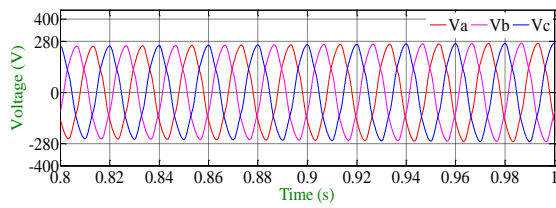

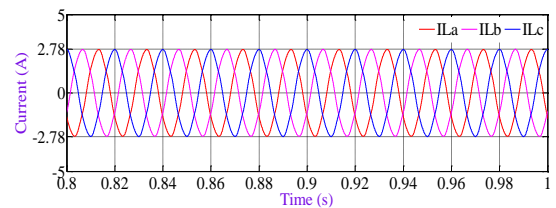Figure 12. Output voltage of inverter with R–load
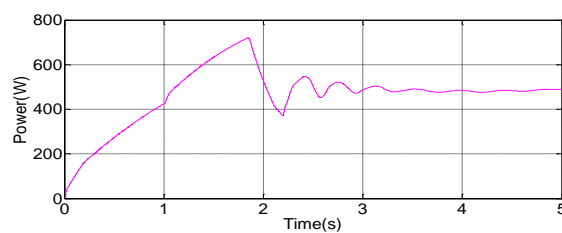

Figure 13. Current through R–load with PRC
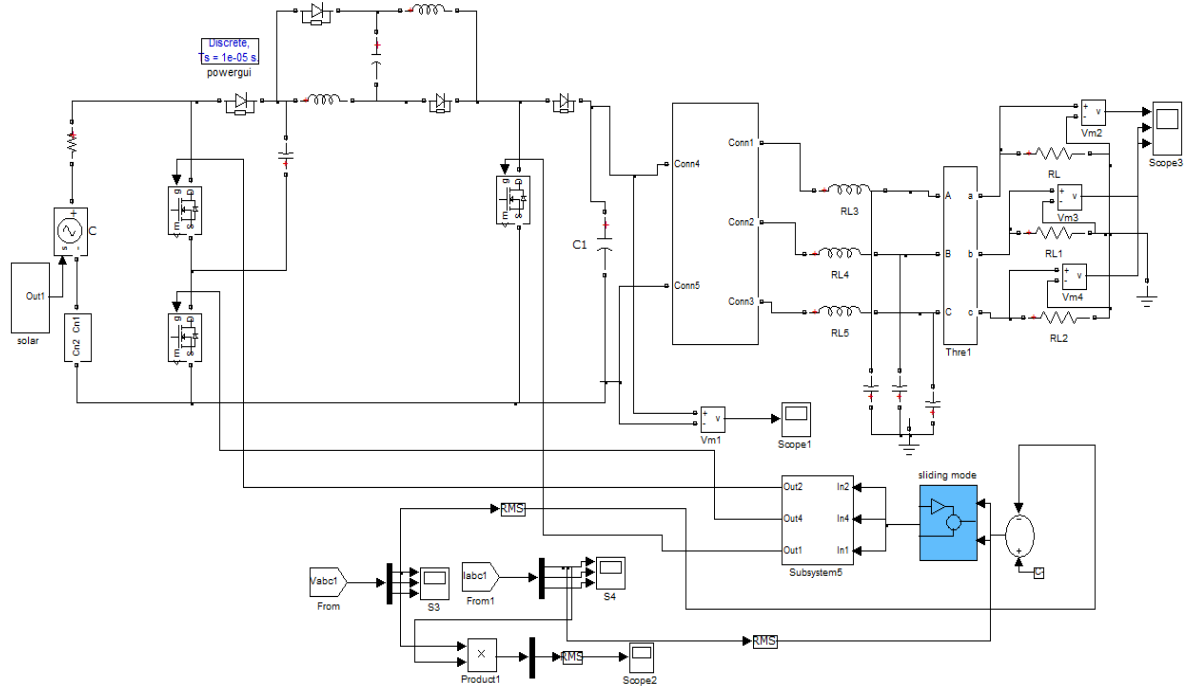

Figure 14. Output power with PRC

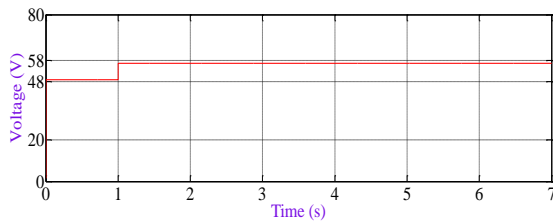Figure 15. Circuit diagram of closed-loop SM controlled BC-TPI
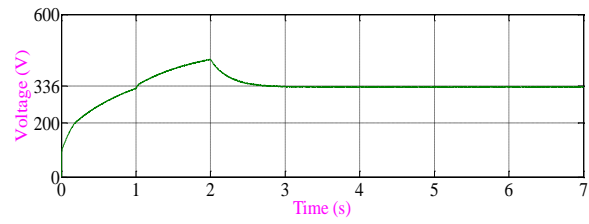

Figure 16. Voltage across PV of BC-TPI
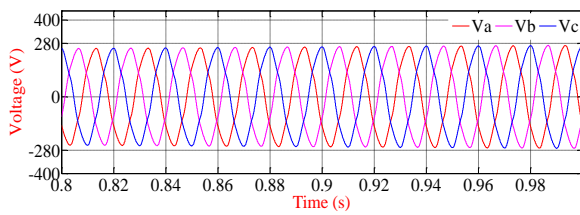

Figure 17. Voltage across BC-TPI

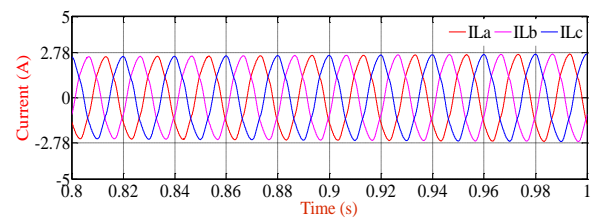
Figure 18. Output voltage of inverter with R–load
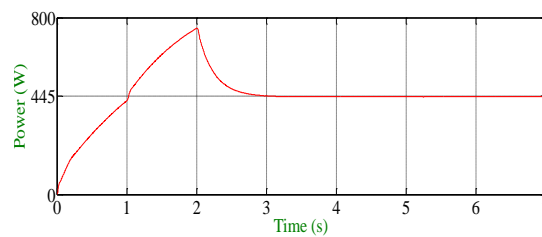

Figure 19. Current through R–load

Figure 20. Output power of BC-TPI

4.   RESULT ANALYSIS

The simulation results of SMC and PRC performed on the BS-TPIS are presented in this section. This section also includes a detailed comparison of both control strategies to system performance. Table 2 provides a quantitative summary of the performance characteristics of the BS-TPI between SMC and PRC. According to the data in Table 2, SMC has the quickest settling time (T_s) of 2.65 sec and PR controller requires an additional 0.55 sec. In comparison, the PRC has the highest maximum peak time (T_p) of 1.84 sec and the SMC has the lowest value of the two controllers. SMC has the fastest rise time (T_r) of 1.27 sec, while PRC requires an extra time. Also in comparison, the SMC is having the less steady state error (ESS) of 1.67 than the PRC.

Table 2. Comparison of time domain parameters

Controller Type	T_r (sec)	T_s (sec)	T_p (sec)	ESS
PRC	1.48	3.20	1.84	2.12
SMC	1.27	2.65	1.78	1.67

5.   CONCLUSION

To simulate the performance comparison of PRC and SMC, Simulink is employed. We compare the output voltage and ripple voltage of the simulation results. The outcomes demonstrate that the SMC works better than the PRC. According to the simulation results, the SMC-based bootstrap BC-TPI results in a shorter settling time and a smaller amount of steady-state inaccuracy. A transformer less connection is possible with the help of a bootstrap converter. By creating a simple method for locating closed-loop controllers for BC-TPI, the current study makes a contribution. It has been determined that the SMC is the best controller for the BC-TPI System. The main advantage of using SMC is the simplicity with which the load voltage can be changed.

REFERENCES

[1]   O. Lopez-Santos, J. C. Mayo-Maldonado, J. C. Rosas-Caro, J. E. Valdez-Resendiz, D. A. Zambrano-Prada, and O. F. Ruiz-Martinez, "Quadratic boost converter with low-output-voltage ripple," *IET Power Electronics*, vol. 13, no. 8, pp. 1605–1612, Jun. 2020, doi: 10.1049/iet-pel.2019.0472.
[2]   V. Narasimhulu, V. Naga Bhaskar Reddy, and Dr. Ch. Sai Babu, "Control of cascaded multilevel inverter by using carrier-based PWM technique and implemented to induction motor drive," *icgst*, vol. 10, no. 1, pp. 11–18, 2010.
[3]   B. J. Kumar and B. Banakara, "Current mode proportional resonant controlled multi input–SEPIC-re-boost-system," *International Journal of Power Electronics and Drive Systems (IJPEDS)*, vol. 10, no. 2, p. 682, Jun. 2019, doi: 10.11591/ijpeds.v10.i2.pp682-689.
[4]   V. Narasimhulu, D. V. Ashok Kumar, and C. Sai Babu, "Fuzzy logic control of SLMMC-based SAPF under nonlinear loads," *International Journal of Fuzzy Systems*, vol. 22, no. 2, pp. 428–437, Mar. 2020, doi: 10.1007/s40815-019-00622-0.
[5]   V. Narasimhulu, D. V. Ashok Kumar, and C. Sai Babu, "Computational intelligence based control of cascaded H-bridge multilevel inverter for shunt active power filter application," *Journal of Ambient Intelligence and Humanized Computing*, Jan. 2020, doi: 10.1007/s12652-019-01660-0.
[6]   V. Narasimhulu, D. V. Ashok Kumar, and C. Sai Babu, "Recital analysis of multilevel cascade H-bridge based active power filter under load variation," *SN Applied Sciences*, vol. 1, no. 12, p. 1621, Dec. 2019, doi: 10.1007/s42452-019-1669-8.
[7]   K. R. Kumar, K. R. Raja, S. Padmanaban, S. M. Muyeen, and B. Khan, "Comprehensive review of KY converter topologies, modulation and control approaches with their applications," *IEEE Access*, vol. 10, pp. 20978–20994, 2022, doi: 10.1109/ACCESS.2022.3151697.
[8]   R. Kannan and S. Srinath, "Performance evaluation of modified high gain step-up converter with enhanced power output and reduced output voltage ripple," in *2018 2nd International Conference on Inventive Systems and Control (ICISC)*, Jan. 2018, pp. 76–80, doi: 10.1109/ICISC.2018.8398935.
[9]   J. Nandha Gopal, N. B. Muthuselvan, and S. Muthukaruppasamy, "Model predictive controller–based quadratic boost converter for WECS applications," *International Transactions on Electrical Energy Systems*, vol. 31, no. 12, Dec. 2021, doi: 10.1002/2050-7038.13133.
[10] N. G. J. and M. N.B., "Current mode fractional order PID control of wind-based quadratic boost converter inverter system with enhanced time response," *Circuit World*, vol. 47, no. 4, pp. 368–381, Oct. 2021, doi: 10.1108/CW-03-2020-0038.
[11] Y. Nagaraja, T. Devaraju, A. Muni Sankar, and V. Narasimhulu, "PV and wind energy conversion exploration based on grid integrated hybrid generation using the cuttlefish algorithm," *Engineering, Technology & Applied Science Research*, vol. 12, no. 6, pp. 9670–9675, 2022, doi: 10.48084/etasr.5364.
[12] S. K. Dash and P. K. Ray, "Power quality improvement utilizing PV fed unified power quality conditioner based on UV-PI and PR-R controller," *CPSS Transactions on Power Electronics and Applications*, vol. 3, no. 3, pp. 243–253, Sep. 2018, doi: 10.24295/CPSSTPEA.2018.00024.
[13] N. Siddharthan and B. Balasubramanian, "Performance analysis of fuzzy logic controlled triple lift configured zeta converter cascaded with inverter fed PMBLDC drive," *Materials Today: Proceedings*, Feb. 2021, doi: 10.1016/j.matpr.2020.12.1055.
[14] V. Narasimhulu, D. V. Ashok Kumar, and C. Sai Babu, "Simulation Analysis of Switch Controlled Power Filters for Harmonic Reduction," *International Journal of Applied Engineering Research*, vol. 11, no. 12, p. 7597, Jun. 2016, doi: 10.37622/IJAER/11.12.2016.7597-7602.
[15] K. Saravanan, L. Porchelvi, and K. Selvakumar, "Hysteresis controlled quadratic boost converter based AC micro grid system

with improved dynamic response," *International Journal of Recent Technology and Engineering*, vol. 8, no. 2 Special Issue 11, pp. 3327–3337, Nov. 2019, doi: 10.35940/ijrte.B1561.0982S1119.

[16] G. Revana and V. R. Kota, "Closed loop fuzzy logic controlled pv based cascaded boost five-level inverter system," *Journal of The Institution of Engineers (India): Series B*, vol. 99, no. 2, pp. 137–145, Apr. 2018, doi: 10.1007/s40031-017-0291-7.

[17] V. Narasimhulu and K. Jithendra Gowd, "Performance analysis of single-stage PV connected three-phase grid system under steady state and dynamic conditions," 2021, pp. 39–46.

[18] K. Jyothi, D. Ravikishore, and H. S. Jain, "Voltage sag mitigation in PV boot-strap converter inverter system," *Journal of Physics: Conference Series*, vol. 1818, no. 1, p. 012228, Mar. 2021, doi: 10.1088/1742-6596/1818/1/012228.

[19] S. Subramanian, C. Sankaralingam, G. Dhiman, and H. Singh, "Hysteretic controlled Inter-leaved buck –converter based AC-DC micro-grid system with enhanced response," *Materials Today: Proceedings*, Mar. 2021, doi: 10.1016/j.matpr.2021.02.087.

[20] R. Elavarasu and C. Christober Asir Rajan, "Closed loop fuzzy logic controlled interleaved DC-to-DC converter fed DC drive system," *International Journal of Engineering & Technology*, vol. 7, no. 2.24, p. 397, Apr. 2018, doi: 10.14419/ijet.v7i2.24.12120.

[21] D. Vanitha and M. Rathinakumar, "Photovoltaic based proportional resonant controlled buck boost converter with coupled inductor," in *2017 IEEE International Conference on Power, Control, Signals and Instrumentation Engineering (ICPCSI)*, Sep. 2017, pp. 1817–1822, doi: 10.1109/ICPCSI.2017.8392029.

[22] N. Janaki and R. Krishna Kumar, "Enhanced 'BDABDC-DC' system for vehicle to grid technology," *International Journal of Recent Technology and Engineering*, vol. 8, no. 2 Special Issue 11, pp. 4021–4025, Nov. 2019, doi: 10.35940/ijrte.B1548.0982S1119.

[23] Shi-Peng Huang, Hua-Qing Xu, and Yan-Fei Liu, "Sliding-mode controlled Cuk switching regulator with fast response and first-order dynamic characteristic," in *20th Annual IEEE Power Electronics Specialists Conference*, pp. 124–129, doi: 10.1109/PESC.1989.48481.

[24] E. Fossas, L. Martinez, and J. Ordinas, "Sliding mode control reduces audiosusceptibility and load perturbation in the Cuk converter," *IEEE Transactions on Circuits and Systems I: Fundamental Theory and Applications*, vol. 39, no. 10, pp. 847–849, 1992, doi: 10.1109/81.199870.

[25] L. Malesani, R. G. Spiazzi, and P. Tenti, "Performance optimization of Cuk converters by sliding-mode control," *IEEE Transactions on Power Electronics*, vol. 10, no. 3, pp. 302–309, May 1995, doi: 10.1109/63.387995.

[26] M. Oppenheimer, I. Husain, M. Elbuluk, and J. A. De Abreu Garcia, "Sliding mode control of the Cuk converter," in *PESC Record. 27th Annual IEEE Power Electronics Specialists Conference*, Aug. 2012, vol. 2, no. 8, pp. 1519–1526, doi: 10.1109/PESC.1996.548783.

[27] J. Mahdavi, "Sliding-mode control of PWM Cuk converter," in *6th International Conference on Power Electronics and Variable Speed Drives*, 1996, vol. 1996, pp. 372–377, doi: 10.1049/cp:19960943.

[28] E. Fossas and A. Ras, "Second-order sliding-mode control of a Buck converter," in *Proceedings of the 41st IEEE Conference on Decision and Control, 2002.*, vol. 1, pp. 346–347, doi: 10.1109/CDC.2002.1184516.

[29] Y. B. Shtessel, A. S. I. Zinober, and I. A. Shkolnikov, "Boost and buck-boost power converters control via sliding modes using method of stable system centre," in *Proceedings of the IEEE Conference on Decision and Control*, 2002, vol. 1, pp. 340–345, doi: 10.1109/cdc.2002.1184515.

[30] A. K and S. K. S, "Closed loop control of DC-DC converters using PID and FOPID controllers," *International Journal of Power Electronics and Drive Systems (IJPEDS)*, vol. 11, no. 3, p. 1323, Sep. 2020, doi: 10.11591/ijpeds.v11.i3.pp1323-1332.

[31] M. I. F. M. Hanif, M. H. Suid, and M. A. Ahmad, "A piecewise affine PI controller for buck converter generated DC motor," *International Journal of Power Electronics and Drive Systems (IJPEDS)*, vol. 10, no. 3, p. 1419, Sep. 2019, doi: 10.11591/ijpeds.v10.i3.pp1419-1426.

[32] A. F. A. Aziz, M. F. Romlie, and T. Z. A. Zulkifli, "CLL/S detuned compensation network for electric vehicles wireless charging application," *International Journal of Power Electronics and Drive Systems (IJPEDS)*, vol. 10, no. 4, p. 2173, Dec. 2019, doi: 10.11591/ijpeds.v10.i4.pp2173-2181.

[33] J. R. Garcia-Sanchez *et al.*, "A robust differential flatness-based tracking control for the 'MIMO DC/DC boost converter– inverter–DC motor' system: sxperimental results," *IEEE Access*, vol. 7, pp. 84497–84505, 2019, doi: 10.1109/ACCESS.2019.2923701.

[34] M. Y. A. Khan, H. Liu, S. Habib, D. Khan, and X. Yuan, "Design and performance evaluation of a step-up DC–DC converter with dual loop controllers for two stages grid connected PV inverter," *Sustainability*, vol. 14, no. 2, p. 811, Jan. 2022, doi: 10.3390/su14020811.

[35] L. Wu, J. Liu, S. Vazquez, and S. K. Mazumder, "Sliding mode control in power converters and drives: a review," *IEEE/CAA Journal of Automatica Sinica*, vol. 9, no. 3, pp. 392–406, Mar. 2022, doi: 10.1109/JAS.2021.1004380.

BIOGRAPHIES OF AUTHORS

Kesa Jyothi 🆔 🅖 SC ◐ worked as an Associate Professor in the Department of Electrical and Electronics Engineering at Vardhaman College of Engineering (Autonomous), Hyderabad, Telangana since 2008 to 2021. She is graduated from KSRM College of Engineering, Sri Venkateswara University, Tirupati, Andhra Pradesh, India. She secured Master of Technology in Electrical Power Engineering, Jawaharlal Nehru Technological University, Hyderabad, India. She is pursuing her Ph.D. in Electrical and Electronics Engineering, Koneru Lakshmaiah Education Foundation, Guntur, Andhra Pradesh India. She is in teaching profession for 13 years. Her main area of interest includes power systems, renewable energy systems, and power electronics. She can be contacted at email: jyothi11.eee@gmail.com.

Pinni Srinivasa Varma 🆔 🔴 SC 🔵 completed his M.Tech and Ph.D. from JNTU Anantapur. His areas of research are Power System Deregulation and Power System Reliability. He has published 35 research papers in various international journals and conferences. He has written a textbook on Power System Deregulation and is published by Lambert publishers. Now, he is working as Associate Professor in Electrical and Electronic Engineering Department, Koneru Lakshmaiah Education Foundation, Guntur, Andhra Pradesh. He can be contacted at email: pinnivarma@kluniversity.in.

Dondapati Ravi Kishore 🆔 🔴 SC 🔵 working as a Professor in the Department of Electrical & Electronics Engineering at Godavari Institute of Engineering & Technology (Autonomous), Rajahmundry. He is graduated from Andhra university, Visakhapatnam, Andhra Pradesh, India. He secured Master of Technology in Energy systems, Jawaharlal Nehru Technological University, Hyderabad, India. He secured Ph.D. in Energy systems, Jawaharlal Nehru Technological University, Hyderabad, India. He is in the field of Electrical & Electronics Engineering as a HOD at GIET (A), Rajahmundry, India. He is in teaching profession for more than 24 years. He has presented 42 papers in National and International Journals, conferences, and Symposiums. His main area of interest includes power systems, renewable energy systems, and energy auditing. He can be contacted at email: dravikishore@gmail.com.

Hari Shankar Jain 🆔 🔴 SC 🔵 is currently engaged as Professor in the Department of Electrical & Electronics Engineering at Vardhaman college of Engineering, Hyderabad. Dr. Jain headed Corporate R&D Division of Bharat Heavy Electrical Limited (BHEL) in the capacity of Executive Director during 2010-12. BHEL is a US $10 billion, Public Sector Undertaking of Indian government producing power plant equipment and products for Industrial/transportation/transmission sectors. As a core electrical engineer Dr. Jain specializes in power systems and apparatus. He coordinated activities of transmission systems group specializing in Gas Insulated Power Equipment and Systems including high voltage switchgear for several years. He is a senior member of IEEE, USA, life member of Magnetic Society of India and has several patents and publications to his credit. He can be contacted at email: jhshankar@gmail.com.